Conformation of Different *S*-Deoxo-Xaa^3-amaninamide Analogues in DMSO Solution as Determined by NMR Spectroscopy. Strong CD Effects Induced by βI, βII Conformational Change

Wolfgang Schmitt,[†] Giancarlo Zanotti,[‡] Theodor Wieland,[§,⊥] and Horst Kessler*[,†]

Contribution from the Institut für Organische Chemie und Biochemie, Technische Universität München, Germany, Centro di Chimica del Farmaco del CNR, Dipartimento di Studi Farmaceutici, Università 'La Sapienza', Roma, Italy, and Max-Planck Institut für medizinische Forschung, Heidelberg, Germany

Received August 28, 1995[⊗]

Abstract: The amatoxines form a class of naturally occurring bicyclic octapeptides responsible for the poisonous effect of *Amanita* mushrooms. For the investigation of structure−activity relationships many derivatives of these peptides have been synthesized and tested up to now. To examine the particular role of the configuration of the amino acid in position 3, three new analogues of *S*-deoxo-amaninamide have been synthesized in which residue 3 is replaced by L-Ala, D-Ala, or Gly. CD spectra in methanol show large deviations which indicate conformational differences or isomeric bridging during synthesis. To discriminate both possibilities a detailed NMR analysis was performed. The conformation of these compounds has been determined in DMSO solution by highfield NMR spectroscopy, distance geometry, and molecular dynamic calculations. The resulting structures are surprisingly similar and closely related to the *x*-ray structure of β-amanitin: Conformational differences are only found in the turn region of Hyp^2-Xaa^3. Hence, the strong differences of the CD spectra rise only from type I/type II variations of this β-turn.

Introduction

Most of the deadly mushroom intoxications are caused by ingestion of *Amanita phalloides* or *Amanita virosa*. These mushrooms contain three different classes of toxins.[1,2] Phallotoxins (bicyclic heptapeptides) and virotoxins (monocylic heptapeptides) are quick acting substances which cause death of white mice in 2−4 h after parenteral administration.[3,4] They act on liver cells where they bind strongly to F-actin.[2,5] This results in a weakening of the plasma membrane and leads to the appearance of vacuoles filled with blood. As a consequence the liver swells and the amount of the circulating blood is thus reduced by 60−65%, and the organism dies due to haemodynamic shock. A third class of toxic peptides are the slowly acting amatoxins (bicyclic octapeptides) which exhibit LD_{50} values up to ten times lower, depending on the animal species, than the other two kinds of toxins mentioned above. The amatoxins are the peptides responsible for the intoxicating effect after ingestion of *A. phalloides*. They lead to death after 4−8 days.[3] Amatoxins bind very selectively to the 140 kDa subunit (SB3) of DNA-dependent RNA polymerase B in nuclei of all eukariontic cells.[6] A very stable ternary complex of toxin, polymerase, DNA template, and the nascent mRNA is formed.[7,8] After the first phosphodiester bond is built the translocation of the polymerase along the DNA template, and therefore the synthesis of mRNA and so protein synthesis is blocked.[2,8]

To date nine different naturally occurring peptides of the amatoxin family have been isolated;[1−3] their chemical structures are shown in Table 1. They all exhibit the same bicyclic framework which is important for their activity (see Figure 1).

To investigate structure−activity relationships on the inhibitory action of these toxins more then 40 different analogues have been synthesized.[1−3,9] One result is the importance of the chemical nature of the side chain in position 3.[2,3,9,10] Therefore, three new analogues of *S*-deoxo-amaninamide containing either Ala, D-Ala, or Gly instead of residue 3 have been synthesized to evaluate the influence of the chirality at this position.

The CD spectra of these three analogues differ dramatically in the region of 210−260 nm (see Figure 2). The L-Ala^3 analog (**1**) shows negative values in this region, and the curve of the D-Ala^3 analog (**2**) is always positive, while the spectrum of the Gly^3 analog (**3**) lies in-between. This was interpreted as an indication of conformational differences between these compounds in solution. For this class of bicyclic peptides theoretically two different diastereomers are possible: a normal form and the related iso-form (see Figure 3). The sulfide bridge can be formed either above (normal) or below the cyclic peptide backbone. In comparison with the CD spectra of *S*-deoxo-D-Ile^3-amaninamide (number **4** in ref 10), where both of these isomers could be isolated, the spectrum of **1** resembles that of the normal form of **4**, while **2** shows a similar curvature as iso-

[†] Technische Universität München.
[‡] Università 'La Sapienza'.
[§] Max-Planck Institut für medizinische Forschung.
[⊥] Deceased November 24, 1995.
[⊗] Abstract published in *Advance ACS Abstracts,* April 15, 1996.

(1) Wieland, Th. *Peptides of the Poisonous Amanita Mushrooms*; Springer Verlag, New York, 1986.
(2) Wieland, Th. *Int. J. Peptide Protein Res.* **1983**, *22*, 257−276.
(3) Wieland, Th.; Faulstich, H. *CRC Crit. Rev. Biochem.* **1978**, *5*, 185−260.
(4) Faulstich, H.; Baku, A.; Bodenmüller, H.; Wieland, Th. *Biochemistry* **1980**, *19*, 3334−3343.
(5) Faulstich, H.; Schäfer, A. J.; Weckauf, M. *Hoppe-Seyler's Z. Physiol. Chem.* **1977**, *358*, 181−184.
(6) Brodner, O. G.; Wieland, Th. *Biochemistry* **1976**, *15*, 3480−3484.
(7) Cochet-Meilhac, M.; Chambon, P. *Biochim. Biophys. Acta* **1974**, *353*, 160−184.
(8) Vaisius, A. C.; Wieland, Th. *Biochemistry* **1982**, *21*, 3097−3101.
(9) Wieland, Th.; Götzendorfer, C.; Zanotti, G.; Vaisius, A. C. *Eur. J. Biochem.* **1981**, *117*, 161−164.
(10) Zanotti, G.; Petersen, G.; Wieland, Th. *Int. J. Peptide Protein Res.* **1992**, *40*, 551−558.

S0002-7863(95)02970-2 CCC: $12.00

Table 1. Naturally Occurring and Synthetic Amatoxins

compound	R^1	R^2	R^3	R^4	X
α-amanitin	NH_2	OH	$CH(CH_3)CH(OH)CH_2OH$	OH	SO
β-amanitin	OH	OH	$CH(CH_3)CH(OH)CH_2OH$	OH	SO
γ-amanitin	NH_2	OH	$CH(CH_3)CH(OH)CH_3$	OH	SO
ϵ-amanitin	OH	OH	$CH(CH_3)CH(OH)CH_3$	OH	SO
amanin	OH	OH	$CH(CH_3)CH(OH)CH_2OH$	H	SO
amaninamide	NH_2	OH	$CH(CH_3)CH(OH)CH_2OH$	H	SO
amanullin	NH_2	OH	$CH(CH_3)CH_2CH_3$	OH	SO
amanullic acid	OH	OH	$CH(CH_3)CH_2CH_3$	OH	SO
proamanullin	NH_2	H	$CH(CH_3)CH_2CH_3$	OH	SO
S-deoxo-Ala³-amaninamide **1**	NH_2	OH	CH_3 (l)	OH	S
S-deoxo-D-Ala³-amaninamide **2**	NH_2	OH	CH_3 (d)	OH	S
S-deoxo-Gly³-amaninamide **3**	NH_2	OH	H	OH	S

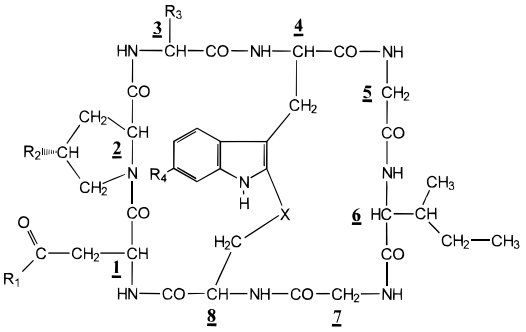

Figure 1. General structure of the amatoxin-peptides; the different substituents are listed in Table 1.

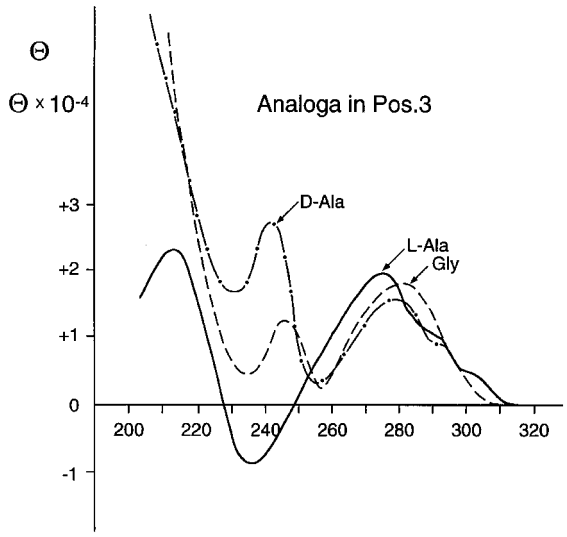

Figure 2. CD spectra of the three analogues: *S*-deoxo-Ala³-amaninamide (solid line), *S*-deoxo-D-Ala³-amaninamide (dotted line) and *S*-deoxo-Gly³-amaninamide (dashed line).

4.[10] Hence, one could draw the conclusion that **1** exhibits a conformation analogous to the normal form and **2** exists in the iso-form. This assumption should be proven by careful conformational analysis in solution using NMR spectroscopy.

Experimental Methods

Synthesis. The amino acids, other chemicals, and solvents were of analytical grade. Analysis by TLC was performed on silica (Merck 60 F 254) using the solvent mixtures indicated for each substance. Detection of the substances on TLC plates was feasible as dark spots on illumination with UV. The inhibitory capacities were tested with an enzyme preparation from embryos of *Drosophila melanogaster* in the laboratory of E.K.F. Bautz, Heidelberg.

Abbreviations. iBCCl, isobutyloxycarbonylchloride; Boc, *tert*-butyloxycarbonyl; DCCI, dicyclohexylcarbodiimide; Ddz, α,α-dimethyl-3,5-dimethoxybenzyloxycarbonyl; DMF, dimethylformamide; DMSO, dimethyl sulfoxide; Hpi, L-3a-hydroxy-1,2,3,3a,8,8a-hexahydropyrrolo-(2,3-*b*)-indole-2-carboxylic acid; HOBt, hydroxybenzotriazole; MA, mixed anhydride; NMM, *N*-methylmorpholine; TLC, thin layer chromatography; TFA, trifluoroacetic acid; THF, tetrahydrofurane.

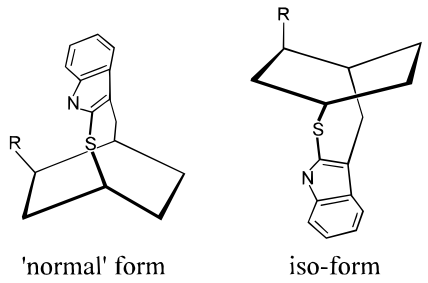

Figure 3. Schematic drawing of the two possible isomers for amatoxins.

Ddz-Hyp-D-Ala-OtBu (2.1). To the solution of 1.28 g (5 mmol) of Ddz-Hyp-OH in 50 mL of CH_2Cl_2 were added at −10 °C under stirring 0.68 g (5 mmol) of iBCCl and 0.68 g (6.7 mmol) of NMM. After 10 min the solution of 0.725 g (5 mmol) of H-D-Ala-OtBu in 20 mL of CH_2Cl_2 was added, and the reaction mixture was kept 3 h at room temperature, washed with aqueous $NaHCO_3$ solution, 0.5 M $KHSO_4$, and water, dried over Na_2SO_4, and evaporated to give 2.15 g (89% yield) of pure title compound. $R_f = 0.7$ in ethyl acetate.

Ddz-Asn-Hyp-D-Ala-OtBu (2.2). The solution of 2.15 g (4.48 mmol) of Ddz-Hyp-D-Ala-OtBu (**2.1**) in a mixture of 3.42 mL of TFA and 150 mL of CH_2Cl_2 was stirred at room temperature for 20 min then extracted with aqueous $NaHCO_3$ and water and dried over Na_2SO_4. This solution was mixed with a solution of 1.58 g (4.48 mmol) of Ddz-Asn-OH and 1.20 g (8.96 mmol) of HOBt in 20 mL of DMF, cooled to 0 °C, and combined with a solution of 0.920 g (4.48 mmol) of DCCI in 20 mL of DMF. After stirring for 1 h at 0 °C and overnight at room temperature, the solvent was evaporated in vacuo, and the residue was dissolved in ethyl acetate. The solution, cleared from dicyclohexylurea and worked up as described in the previous paragraph, gave a residue which was chromatographed on a Sephadex LH 20 column (5 cm × 250 cm) in methanol as eluent, yielding 0.82 g (30%) of **2.2**. $R_f = 0.25$ in ethyl acetate.

Boc-Hpi-Gly-Ile-Gly-Cys(STrt)-Asn-Hyp-D-Ala-OtBu (2.3). The solution of 0.82 g (1.38 mmol) of **2.2** in a mixture of 1.05 mL of TFA and 40 mL of CH_2Cl_2 was stirred at room temperature for 20 min and neutralized with NMM. This precooled solution was added after 8 min to a MA solution prepared at −10 °C from 1.23 g (1.38 mmol) of Boc-Hpi-Gly-Ile-Gly-Cys(STrt)-OH in 30 mL of THF with 0.168 g (1.38 mmol) of iBCCl and 0.168 g (1.66 mmol) of NMM. After 3 h stirring at room temperature the reaction mixture was worked up as described for analogous cases. Peptide **2.3** was obtained by chromatography with methanol in a 2.5 cm × 250 cm column of Sephadex LH 20. Fractions (25 mL) 35−40 afforded 0.98 g (57% yield) of title compound. $R_f = 0.5$ in ethyl acetate−methanol 9:1.

2-Mercapto-L-tryptophylglycyl-L-isoleucylglycyl-L-cysteinyl-L-asparaginyl-*trans*-hydroxy-L-prolyl-D-alanine Cyclic (1→5) Sulfide (2.4). The solution of 0.98 g (0.78 mmol) of octapeptide **2.3** in 250 mL of TFA was kept at room temperature for 3 h and evaporated in vacuo. The residue was washed thoroughly with diethyl ether and

chromatographed on a Sephadex LH 20 column (5 cm × 150 cm) in aqueous 0.004 N NH_4OH as eluent. Fractions (30 mL) 31−40 afforded 0.3 g (46% yield) of seco-thioether **2.4**. $R_f = 0.3$ in *n*-butanol−acetic acid−water 4:1:1.

Cyclic(L-asparaginyl-*trans*-hydroxy-L-prolyl-D-alanyl-L-tryptophylglycyl-L-isoleucylglycyl-L-cysteinyl) (4→8) Sulfide (2). The solution of 0.3 g (0.42 mmol) of **2.4** in 80 mL of THF and 150 mL of DMF was treated at −10 °C under stirring with 34 mg of TFA and 5 min later with 41 mg of iBBCI. After 10 min stirring at the same temperature, the precooled solution of 100 mg of NMM in 240 mL of THF and 450 mL of DMF was added. After standing 1 h at 0 °C and overnight at room temperature, the solution was evaporated in vacuo, and the residue was chromatographed on a silica gel column (2.5 cm × 50 cm) in $CHCl_3-CH_3OH-H_2O$ (65:25:4) as eluent. The residue obtained from fractions (15 mL) 25−35 was further purified by HPLC in a CH_3CN-H_2O gradient yielding 80 mg (23%) of title compound. $R_f = 0.8$ in $CHCl_3-CH_3OH-H_2O$ 65:25:4.

Mass spectrum measurement (FAB) of $(M + H)^+$ exhibited a mass of 813 as expected.

Ddz-Hyp-Gly-OtBu (3.1). To the solution of 1.6 g (4 mmol) of Ddz-Hyp-OH in 30 mL of CH_2Cl_2 were added at −10 °C under stirring 0.544 g (4 mmol) of iBCCl and 0.544 g (5.4 mmol) of NMM. After 10 min the solution of 0.52 g (4 mmol) of H-Gly-OtBu in 20 mL of CH_2Cl_2 was added. After 3 h stirring at room temperature the reaction mixture, worked up as usual, gave 1.6 g (85% yield) of **3.1**. $R_f = 0.6$ in ethyl acetate.

Ddz-Asn-Hyp-Gly-OtBu (3.2). The solution of 1.6 g (3.43 mmol) of Ddz-Hyp-Gly-OtBu in a mixture of 2.6 mL of TFA and 100 mL of CH_2Cl_2 was stirred at room temperature for 20 min, neutralized with NMM, and mixed at 0 °C with a solution of 1.2 g (3.43 mmol) of Ddz-Asn-OH, 0.926 g (6.86 mmol) HOBt and 0.7 g (3.43 mmol) DCCI in 40 mL of DMF. After stirring 1 h at 0 °C and overnight at room temperature, the reaction mixture, worked up as described in the previous paragraphs, gave a residue which was chromatographed on a Sephadex LH 20 column (5 cm × 250 cm) in methanol yielding 1 g (50%) of **3.2**. $R_f = 0.2$ in ethyl acetate.

Boc-Hpi-Gly-Ile-Gly-Cys(STrt)-Asn-Hyp-Gly-OtBu (3.3). The solution of 1 g (1.7 mmol) of **3.2** in mixture of 1.3 mL of TFA and 50 mL of CH_2Cl_2 was stirred for 20 min at room temperature, neutralized with NMM, and added after 8 min to a MA solution prepared at −10 °C from 1.5 g (1.7 mmol) Boc-Hpi-Gly-Ile-Gly-Cys(STrt)-OH in 30 mL of THF with 0.23 g (1.7 mmol) of iBCCl and 0.23 g (**2.3** mmol) of NMM. After 3 h stirring at room temperature the reaction mixture, worked up as usual, gave a residue which was chromatographed on a Sephadex LH 20 column (5 cm × 250 cm) in methanol. Fractions (30 mL) 98−105 afforded 0.93 g (47% yield) of title compound. $R_f =$ 0.4 in ethyl acetate−methanol 9:1.

2-Mercapto-L-tryptophylglycyl-L-isoleucylglycyl-L-cysteinyl-L-asparaginyl-*trans*-hydroxy-L-prolylglycine Cyclic (1→5) Sulfide (3.4). The solution of 0.93 g (0.75 mmol) of octapeptide **3.3** in 250 mL of TFA was kept 3 h at room temperature, and the residue of the evaporation was washed with diethyl ether and chromatographed on a Sephadex LH 20 column (5 cm × 150 cm) in 0.004 N NH_4OH. Fractions (30 mL) 35−45 yielded 0.38 g (63%) of **3.4**. $R_f = 0.25$ in *n*-butanol−acetic acid−water 4:1:1.

Cyclic(L-asparaginyl-*trans*-hydroxy-L-prolylglycyl-L-tryptophylglycyl-L-isoleucylglycyl-L-cysteinyl) (4→8) Sulfide (3). To the stirred solution of 0.38 g (0.47 mmol) of **3.4** in 125 mL of THF and 250 mL of DMF were added at −10 °C 54 mg of TFA and 5 min later 64 mg of iBCCl. After 10 min stirring at −10 °C the precooled solution of 100 mg of NMM in 300 mL of THF and 600 mL of DMF was added. After stirring 1 h at 0 °C and overnight at room temperature, the reaction, worked up as previously described, gave a residue which was chromatographed on a silica gel column (2.5 cm × 50 cm) in $CHCl_3-CH_3OH-H_2O$ 65:25:4. The residue obtained from fractions (7 mL) 20−32 was further purified by HPLC in a CH_3CN-H_2O gradient yielding 90 mg (24%) of title compound. $R_f = 0.7$ in $CHCl_3-CH_3OH-H_2O$ 65:25:4.

Mass spectrum measurement (FAB) of $(M+H)^+$ exhibited a mass of 799 as expected.

CD Spectra. Circular dichroism (CD) measurements were carried out in methanolic solutions on a Jasco J-600 instrument with appropriate quartz cell.

NMR Measurements. Proton and carbon spectra have been recorded on a Bruker AMX-500 at 500 MHz. Data were processed on a Bruker X32 workstation using the Uxnmr program. All spectra were recorded at a temperature of 300 K, except for the temperature coefficients, which were measured for the amide proton resonances by variation of the temperature from 300 to 325 K. The sample concentration of **1** was 20 mM in DMSO-d_6, that of compound **2** was 15 mM, and that of **3** was 5 mM. All samples were vacuum-sealed after three freeze−thaw−pump cycles. The spectra were calibrated relative to DMSO-d_6 (^{1}H: 2.49 ppm, ^{13}C: 39.5 ppm) as internal standard.

The z-filtered TOCSY spectra[11,12] for **1** and **2** were recorded with 4096 data points in t_2 and 512 data points in t_1 with a relaxation delay of 1 s and a spinlock mixing time of 80 ms using a 10 kHz DIPSI sequence (64 scans). The spectrum of **3** was recorded under the same conditions, but with 430 t_1 increments and 128 scans per increment. For processing a $\pi/2$ shifted squared sine bell was used prior to Fourier transformation in both dimensions.

P.E. COSY spectra[13] were recorded with 8192 data points in t_2 and 512 in t_1 with a relaxation delay of 1 s using a 37° read pulse and 16, 23, and 64 scans for compound **1**, **2**, and **3**, respectively. For the one-dimensional reference spectra 16 384 data points were acquired using the same number of scans as in the 2D spectra and a delay of 4.5 μs before acquisition. A $\pi/2$ shifted squared sine bell apodization was applied in both dimensions before phase-sensitive Fourier transformation (TPPI).

For the carbon assignment HMQC spectra[14−16] using a BIRD sequence for ^{12}CH presaturation[17,18] and GARP-decoupling during acquisition with 2048 data points in t_2 and 512 (**1** and **2**) or 256 (**3**) increments in t_1 were recorded with a relaxation delay of 192 ms and 16 (**1**), 32 (**2**) or 96 (**3**) scans. The signal after the BIRD sequence was minimized with a delay of 198 ms. Additionally HMQC-TOCSY spectra[19] using a 10 kHz MLEV-17 spinlock[20] with a mixing time of 80 ms were acquired with 16 scans for compound **1** and 64 scans for **2**. The first t_1 increment used was calculated according to (4·IN0-180°[^{1}H]-1.28·90°[^{13}C])/2 to obtain a phase correction of 180° (zero order) and −360° (first order) in t_1.[21] The spectra were processed by Fourier transformation after the application of a $\pi/2$ shifted squared sine bell apodization.

The HMBC spectra[22] were recorded with 4096 data points in t_2 and 384 points in t_1 with a relaxation delay of 1 s and a 60 ms delay for the evolution of the long-range coupling with 160 (**1** and **2**) and 224 scans (**3**). To increase the resolution in t_1, the carbonyl resonances were folded back.[21] The first t_1 increment was calculated according to (4·IN0−180°[^{1}H]-1.28·90°[^{13}C])/2 for a proper phasing of folded and nonfolded resonances.

HETLOC spectra[23−25] for **1** and **2** were recorded with 192 respectively 256 scans, 4096 points in t_2 and 512 point in t_1 using a relaxation delay of 1 s and a delay of 198 ms for minimization of signals from

(11) Titman, J. J.; Neuhaus, D.; Keeler, J. *J. Magn. Reson.* **1989**, *85*, 111−131.
(12) Titman, J. J.; Keeler, J. *J. Magn. Reson.* **1990**, *89*, 640−646.
(13) Mueller, L. *J. Magn. Reson.* **1987**, *72*, 191−196.
(14) Mueller, L. *J. Am. Chem. Soc.* **1979**, *101*, 4481−4484.
(15) Bendall, M. R.; Pegg, D. T.; Doddrell, D. M. *J. Magn. Reson.* **1983**, *52*, 81−117.
(16) Bax, A.; Griffey, R. H.; Hawkins, B. L. *J. Magn. Reson.* **1983**, *55*, 301−315.
(17) Bax, A.; Subramanian, S. *J. Magn. Reson.* **1986**, *67*, 565−569.
(18) Byrd, R. A.; Summers, M. F.; Zon, G.; Spellmeyer Fouts, C.; Marzilli, L. G. *J. Am. Chem. Soc.* **1986**, *108*, 504−505.
(19) Lerner, A.; Bax, A. *J. Magn. Reson.* **1986**, *69*, 375−380.
(20) Bax, A.; Davis, D. G. *J. Magn. Reson.* **1985**, *65*, 355−360.
(21) Schmieder, P.; Kessler, H. *Magn. Reson. Chem.* **1991**, *29*, 375−380.
(22) Bax, A.; Summers, M. F. *J. Am. Chem. Soc.* **1986**, *108*, 2093−2094.
(23) Kurz, M.; Schmieder, P.; Kessler, H. *Angew. Chem., Int. Ed. Engl.* **1991**, *30*, 1329−1330.
(24) Schmieder, P.; Kurz, M.; Kessler, H. *J. Biomol. NMR* **1991**, *1*, 403−420.
(25) Wollborn, U.; Leibfritz, D. *J. Magn. Reson.* **1992**, *98*, 142−146.

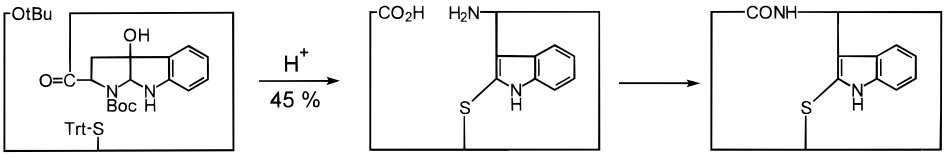

Figure 4. Formation of the first ring of analogs **1**−**3** by the Savige−Fontana reaction and cyclization to yield the bicyclic octapeptides.

the BIRD sequence. The mixing time of the 10 kHz MLEV-17 spinlock used was 40 ms. The complementary spectrum of **3** was recorded with 300 t_1 increments and 656 scans.

For the determination of proton−proton distances NOESY spectra[26] with a mixing time of 200 ms, a relaxation delay of 1 s and 4096 respectively 512 data points in t_2 and t_1 have been recorded. In addition NOESY and ROESY spectra with shorter mixing times were recorded to ensure the lack of spin diffusion. The spectra were processed by applying a $\pi/2$ shifted squared sinebell in both dimensions and zero filling to 1024 complex points in t_1 before phase-sensitive Fourier transformation. The integral intensities were measured using the integral subroutine within the Uxnmr software. The resulting crosspeak volumes were transformed into distances using the isolated two-spin approximation with reference to the Hyp²-H$^{\beta}$,H$^{\beta}$-crosspeak which was set to a distance of 178 pm.

Structure Calculations. A Silicon Graphics Indy with R4400 processor was used for all calculations. The distance geometry calculations were carried out using a modified version of the Disgeo program.[27,28] For each compound 100 structures were embedded into the four-dimensional Cartesian space. These structures were minimized for 400 steps with the steepest descent algorithm followed by 5 ps distance driven dynamics (DDD)[29,30] at 300 K using NOEs and chiral volumes as restraints and 4 ps DDD with a weak coupling to a temperature bath of 1 K. After projection into the three-dimensional space 100 steps of steepest descent minimization using chiral volumes as restraints were performed to relax steric strain. Finally a distance and angle driven dynamic calculation (DADD)[31] was carried out for 5 ps at a temperature of 500 K and subsequently with a weak temperature coupling at 1 K using NOEs, ^3J-coupling constants and chiral volumes as restraints. For the following molecular dynamic simulations a modified version of the Gromos software[32] was used, to permit additionally the inclusion of coupling constants as restraints. The structure of each compound with the lowest total error resulting from the DG calculations was chosen as a starting structure. It was placed in a truncated octahedron ($a = b = c =$ 3.43415 (**1**), 3.42954 (**2**) and 3.28463 nm (**3**)) and soaked with 143 to 164 DMSO molecules. The system was relaxed by using a maximum of 2000 steps with the steepest descent algorithm and a force constant for the NOEs of 2000 kJ/(mol·nm²). In the first step only the solvent was relaxed while the peptide was held fixed. In the second step the whole system was relaxed. The dynamic simulations were performed using the Shake algorithm[33] with a stepsize of 1 fs. The temperature relaxation time was 10 fs, the nonbonded interactions were updated every 10 steps with a cutoff distance of 0.8 nm. The upper and lower bounds for NOEs are set to plus and minus 10% of the experimentally determined distances. Force constants for NOEs and coupling constants were set to 2000 kJ/(mol·nm²) and 0.25 kJ/mol, respectively. For equilibration the first 5 ps were calculated with a strong temperature coupling at 100 K and the next 5 ps at 200 K. The trajectory used for analysis was calculated for 180 ps at 300 K, and a structure was stored every 1000 fs.

The test calculations were performed in vacuo with the Gromos program using NOEs and coupling constants as restraints ($k_{NOE} = 2000$ kJ/(mol·nm²), $k_J = 0.25$ kJ/mol). The starting structures were manually built using the Biopolymer module of the InsightII program (BIOSYM).[34] These structures were optimized by molecular dynamic calculations for 2 ps at 1000 K, 2 ps at 500 K, and finally for 5 ps at 300 K. The trajectories were then recorded for 50 ps at a temperature of 300 K.

Results

The synthesis of the amanitin analogs followed the route described in ref 10. As depicted in Figure 4 the respective N-terminal l-Hpi-octapeptide is subjected to the indole-2-thioether forming Savige-Fontana reaction, and the monocyclic tryptophan octapeptide so obtained is converted to the bicyclic amatoxin analog by internal peptide bond formation. The synthesis of analog **1** has already been published (number **1i** in ref 35).

The assignment of all proton and carbon shifts was performed following a standard strategy previously described.[36−39] Sequential assignment was carried out using heteronuclear long range couplings from HMBC experiments. Proton chemical shifts are listed in Table 2; carbon chemical shifts are available as supporting information. For all of the three compounds only one single conformation in DMSO solution was detected. Hence, no cis−trans isomerization occurs under measurement conditions. The proton chemical shifts of the three analogues are quite similar and each exhibits good dispersion. Other than the signals from residue 3 only few differences in proton shifts can be detected. The resonance of Asn¹-H^N in **1** is shifted 0.2 ppm downfield with respect to **2** and **3**. Also the β-protons of Asn¹ in compound **1** are shifted about 0.4 ppm downfield relative to **2**. These β-protons are separated by 0.3 ppm in **1** and **2**, but they are degenerated in **3**. A further downfield shift of about 0.7 ppm relative to **2** and **3** is detected for the δ-amide protons of Asn¹ in compound **1**. The separation of the β-protons of Trp⁴ in **1** is smaller than in **2** and **3**. These comparisons give a first hint, that the structural difference between these three analogues should occur in the region of residues 1−4.

The homonuclear $^3J_{HN,H\alpha}$ coupling constants were in most cases extracted from the 1D proton spectra recorded with 16 384 data points. Only those of Trp⁴-H^N and Cys⁸-H^N in compound **1**, of Cys⁸-H^N in **2** and of Gly³-H^N as well as that of Gly⁷-H^N in **3** have been determined from the related P.E. COSY

(26) Jeener, J.; Meier, B. H.; Bachmann, P.; Ernst, R. R. *J. Chem. Phys.* **1979**, *71*, 4546−4553.
(27) Havel, T. F. *Disgeo, Quantum Chemistry Exchange Program;* Exchange No. 507, Indiana University, 1986.
(28) Crippen, G. M.; Havel, T. F. *Distance Geometry and Molecular Conformation*; Research Studies Press LTD.: Taunton, Somerset, UK, 1988.
(29) Kaptein, R.; Boelens, R.; Scheek, R. M., van Gunsteren, W. F. *Biochemistry* **1988**, *27*, 5389−5395.
(30) Kuntz, I. D.; Thomason, J. F.; Oshiro, C. M. *Methods Enzymol.* **1989**, *177*, 159−204.
(31) Mierke, D. F.; Geyer, A.; Kessler, H. *Int. J. Peptide Protein Res.* **1994**, *44*, 325−331.
(32) van Gunsteren, W. F.; Berendsen, H. J. C. *Groningen Molecular Simulation (Gromos) Library Manual*; Biomos, B. V., Eds.; Nijenborgh 16, NL 9747 AG Groningen, 1987.
(33) van Gunsteren, W. F.; Berendsen, H. J. C. *Mol. Phys.* **1977**, *34*, 1311−1321.
(34) InsightII; Biosym Technologies Inc.: San Diego, CA 1993.
(35) Zanotti, G.; Möhringer, C.; Wieland, Th. *Int. J. Peptide Protein Res.* **1987**, *30*, 450−459.
(36) Kessler, H.; Bermel, W.; Müller, A.; Pook, K.-H. In *Peptides: Analysis, Synthesis and Biology*; Udenfried, S., Meienhofer, J., Hruby, V., Eds.; Academic Press: New York, 1985; Vol. 7, pp 437−473.
(37) Wüthrich, K. *NMR of Proteins and Nucleic Acids*; John Wiley & Sons: New York, 1986.
(38) Kessler, H.; Seip, S. In *Two-Dimensional NMR Spectroscopy: Applications for Chemists and Biochemists*; Croasmun, W. R., Carlson, R. M. K., Eds.; VCH Publisher: New York, 1994; pp 619−654.
(39) Kessler, H.; Schmitt, W. in *Encyclopedia of Nuclear Magnetic Resonance*; Grant, D. M., Harris, R. K., Eds.; John Wiley & Sons: New York, 1996, pp 3527−3537.

Table 2. Proton Chemical Shifts [ppm] for the Three *S*-Deoxoamaninamide Analogues in DMSO-d_6

residue	proton	**1**	**2**	**3**
Asn[1]	H^N	8.40	8.17	8.22
	H^α	4.76	4.87	4.84
	$H^{\beta1}$	3.17	2.70	2.73
	$H^{\beta2}$	2.85	2.47	2.72
	$H^{N\delta1}$	8.03	7.27	7.25
	$H^{N\delta2}$	7.38	6.86	7.04
Hyp[2]	H^α	4.29	4.48	4.42
	$H^{\beta1}$	2.20	2.06	2.11
	$H^{\beta2}$	1.89	1.90	1.90
	H^γ	4.39	4.45	4.44
	H^{OH}	5.25	5.31	5.29
	$H^{\delta1}$	3.81	3.64	3.69
	$H^{\delta2}$	3.73	3.63	3.69
Xaa[3]	H^N	8.27	8.90	8.84
	H^α	4.31	4.36	3.89 ($H^{\alpha1}$)
	H^β	1.35	1.28	3.66 ($H^{\alpha2}$)
Trp[4]	H^N	7.83	8.10	8.03
	H^α	4.93	4.83	4.92
	$H^{\beta1}$	3.28	3.71	3.57
	$H^{\beta2}$	3.01	2.83	2.90
	$H^{N\epsilon1}$	11.24	11.21	11.22
	$H^{\epsilon3}$	7.54	7.51	7.51
	H^{Z2}	7.24	7.25	7.25
	H^{Z3}	7.00	7.02	7.02
	H^{CH}	7.10	7.11	7.11
Gly[5]	H^N	8.15	7.70	7.79
	$H^{\alpha1}$	4.08	3.94	3.98
	$H^{\alpha2}$	3.44	3.54	3.51
Ile[6]	H^N	8.51	8.56	8.54
	H^α	3.74	3.83	3.81
	H^β	1.58	1.65	1.63
	$H^{\gamma1,1}$	1.53	1.52	1.53
	$H^{\gamma1,2}$	1.10	1.13	1.12
	$H^{\gamma2(Me)}$	0.77	0.80	0.80
	H^δ	0.81	0.82	0.82
Gly[7]	H^N	8.86	8.85	8.86
	$H^{\alpha1}$	3.93	3.94	3.94
	$H^{\alpha2}$	3.41	3.49	3.45
Cys[8]	H^N	7.80	7.54	7.60
	H^α	4.64	4.62	4.63
	$H^{\beta1}$	3.18	3.33	3.28
	$H^{\beta2}$	2.81	2.96	2.93

crosspeak according to the method of Kim and Prestegard.[40] The heteronuclear $^3J_{HN,C\beta}$ couplings were measured from the HETLOC experiments.[24] Following the procedure proposed by Titman and Keeler,[11,12] the heteronuclear $^3J_{HN,C'}$ and $^3J_{H\alpha,C'}$ *i*-1 are calculated via the traces of HMBC and z-filtered TOCSY spectra. P.E. COSY crosspeaks have been used for the measurement of $^3J_{H\alpha,H\beta}$ coupling constants.[13] For compound **1** 42 coupling constants and for **2** 39 coupling constants were determined, whereas only 28 could be extracted for substance **3**, due to the lower signal to noise ratio in the related heteronuclear spectra (see Tables 3 and 4). With these values the populations of the side-chain rotamers for Asn[1] were calculated using the Pachler equations.[41] In **1** the rotamer with $\chi_1 = +60°$ is predominant (66%), whereas in compound **2** the population of the rotamers $+60°$ and $-60°$ are nearly equivalent. Due to the degeneration of the β-protons in **3** no preferred orientation of the side chain of Asn[1] could be derived. From the homonuclear and the heteronuclear coupling constants diastereotopic assignment of Trp[4] and Cys[8] β-protons was performed. In the course of the calculations the assignment of the prochiral α-protons of glycin residues was also possible as

(40) Kim, Y.; Prestegard, J. H. *J. Magn. Reson.* **1989**, *84*, 9−13.
(41) Pachler, K. G. R. *Spectrochim. Acta* **1964**, *20*, 581−587.

Table 3. Vicinal Coupling Constants Defining the Backbone ϕ-Angle as Determined in DMSO-d_6 at 300 K in [Hz]

residue	**1**	**2**	**3**
Asn[1]	$^3J_{HN,H\alpha} = 3.9$ $^3J_{HN,C'} = 2.7$	$^3J_{HN,H\alpha} = 4.8$ $^3J_{HN,C'} = 1.8$	$^3J_{HN,H\alpha} = 4.6$ $^3J_{HN,C'} = 3.1$ $^3J_{HN,C\beta} = 1.9$
Hyp[2]	$^3J_{H\alpha,C'i-1} = 4.3$		
Xaa[3]	$^3J_{HN,H\alpha} = 8.9$ $^3J_{HN,C\beta} = 1.0$	$^3J_{HN,H\alpha} = 8.6$ $^3J_{HN,C\beta} = 1.4$ $^3J_{H\alpha,C'i-1} = 2.9$	$^3J_{HN,H\alpha proR} = 7.0$ $^3J_{HN,H\alpha proS} = 5.8$ $^3J_{H\alpha proS,C'i-1} = 4.4$
Trp[4]	$^3J_{HN,H\alpha} = 9.1$ $^3J_{HN,C\beta} = 1.1$ $^3J_{H\alpha,C'i-1} = 1.4$	$^3J_{HN,H\alpha} = 9.6$ $^3J_{HN,C\beta} = 1.2$	$^3J_{HN,H\alpha} = 9.8$ $^3J_{HN,C\beta} = 0.3$
Gly[5]	$^3J_{HN,H\alpha proS} = 7.7$ $^3J_{HN,H\alpha proR} = 4.8$ $^3J_{HN,C'} = 3.1$ $^3J_{H\alpha proS,C'i-1} = 4.5$ $^3J_{H\alpha proR,C'i-1} = 3.8$	$^3J_{HN,H\alpha proS} = 6.8$ $^3J_{HN,H\alpha proR} = 2.5$ $^3J_{H\alpha proS,C'i-1} = 5.4$ $^3J_{H\alpha proR,C'i-1} = 5.1$	$^3J_{HN,H\alpha proS} = 6.5$ $^3J_{HN,H\alpha proR} = 2.7$ $^3J_{HN,C'} = 1.7$ $^3J_{H\alpha proR,C'i-1} = 5.0$
Ile[6]	$^3J_{HN,H\alpha} = 5.2$	$^3J_{HN,H\alpha} = 5.7$ $^3J_{HN,C\beta} = 1.3$	$^3J_{HN,H\alpha} = 5.5$
Gly[7]	$^3J_{HN,H\alpha proS} = 7.8$ $^3J_{HN,H\alpha proR} = 4.7$ $^3J_{H\alpha proS,C'i-1} = 2.9$ $^3J_{H\alpha proR,C'i-1} = 5.7$	$^3J_{HN,H\alpha proS} = 6.9$ $^3J_{HN,H\alpha proR} = 4.7$ $^3J_{H\alpha proS,C'i-1} = 3.3$ $^3J_{H\alpha proR,C'i-1} = 5.6$	$^3J_{HN,H\alpha proS} = 7.4$ $^3J_{HN,H\alpha proR} = 4.9$ $^3J_{H\alpha proR,C'i-1} = 5.8$
Cys[8]	$^3J_{HN,H\alpha} = 9.7$ $^3J_{HN,C\beta} = 0.3$ $^3J_{H\alpha,C'i-1} = 4.1$	$^3J_{HN,H\alpha} = 9.2$ $^3J_{HN,C\beta} \sim 0$ $^3J_{HN,C'} = 1.0$ $^3J_{H\alpha,C'i-1} = 4.5$	$^3J_{HN,H\alpha} = 9.4$ $^3J_{HN,C\beta} = 1.0$ $^3J_{HN,C'} = \sim 0$

Table 4. Vicinal Coupling Constants Defining the χ-Angle as Determined in DMSO-d_6 at 300 K in [Hz]

residue	**1**	**2**	**3**
Asn[1]	$^3J_{H\alpha,H\beta proR} = 4.7$ $^3J_{H\alpha,H\beta proS} = 4.2$ $^3J_{C',H\beta proR} = 7.5$ $^3J_{C',H\beta proS} \sim 0$	$^3J_{H\alpha,H\beta proR} = 6.3$ $^3J_{H\alpha,H\beta proS} = 4.1$ $^3J_{C',H\beta proR} = 4.5$ $^3J_{C',H\beta proS} = 5.4$	
Hyp[2]	$^3J_{H\alpha,H\beta proR} = 7.3$ $^3J_{H\alpha,H\beta proS} = 11.5$ $^3J_{C',H\beta proR} = \sim 0$ $^3J_{C',H\beta proS} = 4.5$ $^3J_{H\beta proR,H\gamma} \sim 9$ $^3J_{H\beta proS,H\gamma} = 3.6$ $^3J_{H\gamma,H\delta proS} = 3.2$ $^3J_{H\gamma,H\delta proR} \sim 9$	$^3J_{H\alpha,H\beta proR} = 7.6$ $^3J_{H\alpha,H\beta proS} = 10.1$ $^3J_{C',H\beta proR} = \sim 0$ $^3J_{C',H\beta proS} = 5.4$ $^3J_{H\beta proR,H\gamma} = 8.0$ $^3J_{H\beta proS,H\gamma} = 3.7$	$^3J_{H\alpha,H\beta proR} = 7.3$ $^3J_{H\alpha,H\beta proS} = 10.9$
Trp[4]	$^3J_{H\alpha,H\beta proS} = 13.0$ $^3J_{H\alpha,H\beta proR} = 6.4$ $^3J_{C',H\beta proS} = 3.0$ $^3J_{C',H\beta proR} = 9.0$	$^3J_{H\alpha,H\beta proS} = 12.7$ $^3J_{H\alpha,H\beta proR} = 5.4$ $^3J_{C',H\beta proR} = 8.5$	$^3J_{H\alpha,H\beta proS} = 13.0$ $^3J_{H\alpha,H\beta proR} = 5.7$
Ile[6]	$^3J_{H\alpha,H\beta} = 9.0$	$^3J_{H\alpha,H\beta} = 9.5$	$^3J_{H\alpha,H\beta} = 8.3$
Cys[8]	$^3J_{H\alpha,H\beta proR} = 10.8$ $^3J_{H\alpha,H\beta proS} = 3.3$ $^3J_{C',H\beta proR} = 4.8$ $^3J_{C',H\beta proS} = 7.2$	$^3J_{H\alpha,H\beta proR} = 8.6$ $^3J_{H\alpha,H\beta proS} = 3.7$ $^3J_{C',H\beta proR} = 4.5$ $^3J_{C',H\beta proS} = 6.5$	$^3J_{H\alpha,H\beta proR} = 9.4$ $^3J_{H\alpha,H\beta proS} = 3.0$ $^3J_{C',H\beta proS} = 5.3$

in every structure only one of the two α-protons fulfilled the NOE distance constraints. Subsequent calculations were carried out without pseudoatoms.

A comparison of the temperature coefficients shows major differences among the examined analogues only for the amide protons of residue 3 (see Table 5). This amide proton seems to form an additional hydrogen bond in compound **1**.[42] The determined NOE derived distances, together with the upper and lower limits used for the calculations, are available as supporting information. The NOESY spectra indicate that all peptide bonds have trans configuration, as no strong H^α,H^α crosspeaks were detected.

(42) Llinas M.; Klein, M. P., *J. Am. Chem. Soc.* **1975**, *97*, 4731−4737.

Table 5. Temperature Coefficients Given in [ppb/K] of the Amide Protons of All Three Analogues, Determined in the Range of 300 and 325 K

	1	**2**	**3**
Asn¹-HN	−2.0	−1.5	−1.1
Xaa³-HN	−1.5	−4.0	−2.8
Trp⁴-HN	−1.3	−2.5	−1.6
Gly⁵-HN	−2.0	−0.7	−0.7
Ile⁶-HN	−5.1	−4.8	−4.4
Gly⁷-HN	−4.3	−5.0	−4.5
Cys⁸-HN	−1.7	−1.0	−0.8

Table 6. Dihedral Angles of the Refined Structures of the *S*-Deoxoamaninamides (Means of a 150 ps MD Trajectory)

residue	dihedral	**1**	**2**	**3**
Asn¹	ϕ	−173.3	−162.7	−148.2
	ψ	164.6	150.3	146.3
	χ_1	59.0	−107.9	−57.6
	χ_2	−121.1	138.5	98.6
Hyp²	ϕ	−66.7	−64.3	−65.1
	ψ	12.0	119.1	109.2
	χ_1	−28.3	−27.9	−27.8
	χ_2	41.0	39.1	36.9
	χ_3	−38.9	−35.4	32.4
	χ_4	22.4	18.5	15.6
Xaa³	ϕ	−122.3	104.5	119.9
	ψ	7.0	−18.4	−30.6
Trp⁴	ϕ	−143.5	−91.0	−85.9
	ψ	−38.0	−53.3	−53.6
	χ_1	176.2	176.5	174.0
	χ_2	−127.9	−130.4	−115.4
Gly⁵	ϕ	142.3	160.6	169.8
	ψ	−176.7	−168.8	−175.0
Ile⁶	ϕ	−73.0	−73.0	−68.0
	ψ	117.4	134.9	119.4
	χ_1	−59.2	−55.9	−53.9
	χ_2	159.3	−56.3	157.3
Gly⁷	ϕ	98.8	59.3	65.2
	ψ	9.2	33.8	16.1
Cys⁸	ϕ	−130.4	−131.7	−106.6
	ψ	−78.4	−79.1	−91.5
	χ_1	−174.2	167.3	164.8
	χ_2	178.2	−169.2	−178.2

All calculated distance limits were incorporated as restraints for structure calculation. The coupling constants (for which parameters for the Karplus curves exist) were used directly as restraints, following the method introduced by Kim and Prestegard[43] and improved by Mierke and Kessler.[44−46] Distance geometry calculations on all three analogues converged (RMSD < 100 pm), and the conformations of the 20 structures with the lowest total error were very similar. The RMSD value for the backbone atoms of **1** was 28 pm, that for **2** was 52 pm, and 53 pm for **3**. These results suggest that the structure can be described by one predominant conformation for every analog in solution. Hence, in each case the DG structure with the lowest total error was taken as a starting structure for the subsequent molecular dynamic simulation in solution using NOE values and coupling constants as restraints. Only the last 150 ps of the resulting trajectories were analyzed, the first 30 ps are neglected for equilibration of the structure at the simulation temperature. The averaged and minimized structures for the three compounds are shown in Figure 5.

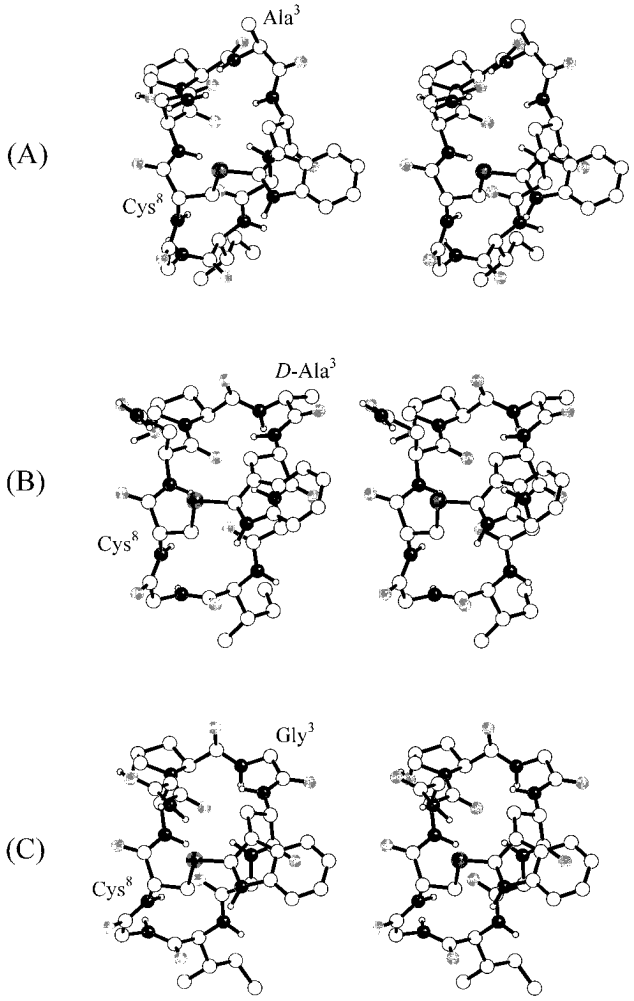

Figure 5. Stereoscopic picture of the conformation of *S*-deoxo-Ala³-amaninamide (**A**), of *S*-deoxo-D-Ala³-amaninamide (**B**) and of *S*-deoxo-Gly³-amaninamide (**C**) in DMSO.

The mean distance restraint violation is low (12 pm for **1** and **2**, 14 pm for **3**) and the resulting dihedral angles (see Table 6) fit to the experimentally measured coupling constants. In all three structures every proton having a low negative temperature coefficient is involved in a hydrogen bond. As the information on hydrogen bond donors was not incorporated into the calculations, the fulfillment of these data is an additional proof for the correctness of the determined structures.

The structure of **1** shows a bent backbone and exhibits the normal form. It has a βII-turn with Ile⁶ in the i+1 position and on the opposite side a βI-turn with Hyp² in the i+1 position. The latter βI-turn is stabilized via an additional hydrogen bond from the Ala³-H^N to the carboxyl oxygen of the Asn¹ side chain. Therefore, the orientation of this side-chain is fixed to a χ_1 angle of +60°, which is in accordance with the analysis of the sidechain rotamer populations. The conformation of the peptide backbone is fixed by additional hydrogen bonds between Asn¹-H^N/Gly⁵-C′ and Gly⁵-H^N/Asn¹-C′. Figure 6 shows the backbone structure of **1** to illustrate the hydrogen bonding network.

The conformation of compound **1** as determined in solution is nearly identical with the X-ray structure of β-amanitin.[47] The RMSD value for the superposition of all backbone atoms is only 22 pm (Figure 7). There are only minor differences in the side-chain orientations, even the stabilization of the βI-turn is the same in both structures.

(43) Kim, Y.; Prestegard, H. *Proteins Struct. Funct. Genet.* **1990**, *8*, 377−385.
(44) Mierke, D. F.; Kessler, H. *Biopolymers* **1993**, *33*, 1003−1017.
(45) Mierke, D. F.; Kessler, H. *Biopolymers* **1992**, *32*, 1277−1282.
(46) Eberstadt, M.; Mierke, D. F.; Köck, M.; Kessler, H. *Helv. Chim. Acta* **1992**, *75*, 2583−2592.
(47) Kostansek, E. C.; Lipscomb, W. N.; Yocum, R. R., Thiessen, W. E. *Biochemistry* **1978**, *17*, 3790−3795.

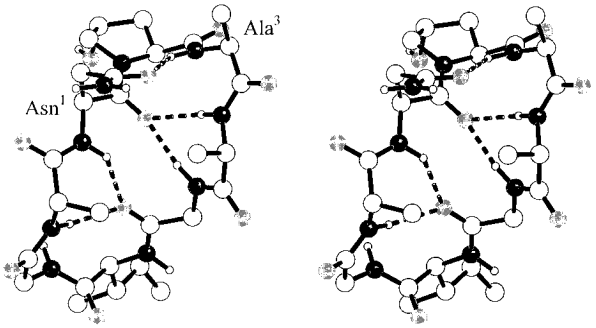

Figure 6. Stereoscopic picture of the backbone conformation of *S*-deoxo-Ala[3]-amaninamide (**3**); hydrogen bonds are painted as dashed lines.

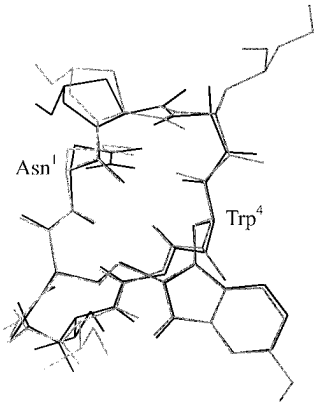

Figure 7. Superposition of the structures of *S*-deoxo-Ala[3]-amaninamide (black line) and β-amanitin (gray line).

The conformation of the analogues **2** and **3** (see Figure 5) is quite similar to that of **1**. The RMSD value for the superposition of all backbone atoms is 22 pm. Both structures show the normal form and exhibit also a bent backbone where both halves are nearly orthogonal to each other. These structures consist of two βII-turns, one with Ile[6] in the $i+1$ and the other one with Hyp[2] in the $i+1$ position.

A comparison of the conformations of all three examined analogues shows that the only difference is found in the structure of the β-turn with Hyp[2] in the $i+1$ position. While the L-Ala[3]-analogue has a βI-turn, which is stabilized through an additional hydrogen bond between Ala[3]-H^N and the carboxyl oxygen of the Asn[1] side chain, the D-Ala[3]- and the Gly[3]-analogue both show a βII-turn (see Figure 8).

The structures of **2** and **3** exhibit the same predominant conformation in solution but not with the same stability. If one compares the temperature coefficients of the amide proton of residue 3; the value for compound **2** (−4.0 ppb/K) indicates a solvent exposed orientation, whereas the value for **3** (−2.8 ppb/K) lies in the border region where both, an internal and an external orientation are possible and that for **1** (−1.5 ppb/K) is typical for the internal orientation of the amide protons. The Xaa[3]-H^N/H^α and the Xaa[3]-H^N/Hyp[2]-H^α distances show the same pattern: the sequential NOE distances are 213 pm (**2**) and 228 pm (**3**), and the interresidual distances are 281 pm (**2**) and 364/332 pm (**3**). Additionally the Xaa[3]-H^N/Trp[4]-H^N distance in **3** is 14 pm shorter than in **2**. The homonuclear $^3J_{HN,H\alpha}$ couplings of residue 3 in the glycin analogue are 7.0 and 5.8 Hz. These data, in particular the coupling constants, indicate that the Gly[3]-analogue is more flexible than the D-Ala[3]-analogue. This is shown by the more averaged values for compound **3** which are not compatible with an absolutely fixed peptide plane between Hyp[2] and Gly[3]. These conformational differences can be explained by allylic 1,3-strain.[48] Due to the repulsion of the carbonyl oxygen of Hyp[2] in compound **1** with the methyl group of Ala[3] an orientation of the amide plane with coplanar arrangement of the oxygen and the α-proton is favored. As the chirality at the α-carbon of residue 3 in compound **2** is inverted an opposite orientation of the amide plain is found. Compound **3** has no side chain in position 3 (Gly). Therefore none of these two orientations of the amide plain is energetically favored. Hence, we suggest that **3** interconverts rapidly on the NMR time scale between the conformation of **1** (βI-turn) and that of **2** (βII-turn).

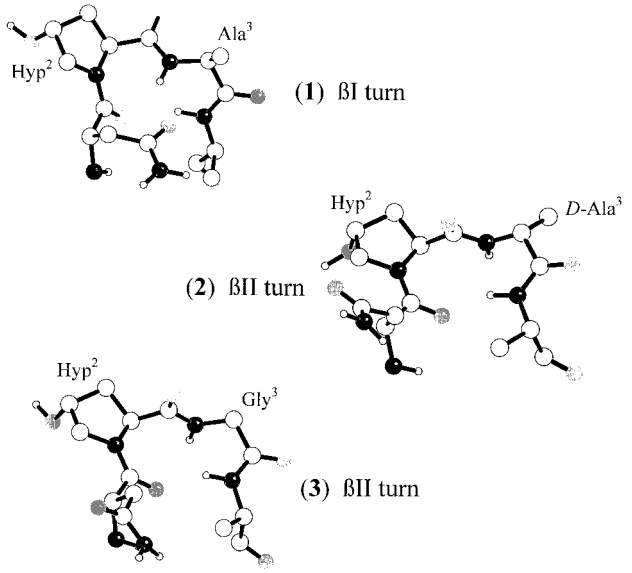

Figure 8. Structures of the turns with Hyp[2] in the $i+1$ position in all three analogues.

A simple comparison of distances within the normal and the iso form to distinguish them is not unambiguous because of conformational differences and easily mislead the interpretation. Hence, detailed calculations taking into account the whole network of distances and coupling constants were performed.

All three analogues show the structure of the normal form in solution even though interchange to the iso-form was allowed during the DG calculations. But the initial assumption, that **2** might exist in the iso form was disproven via additional test calculations. As distance geometry calculations are independent on the starting structure they should lead in every case to the correct isomer. To test this a distance geometry calculation for **2** was performed using the same protocol but *without any restraints*. The resulting structures show a ratio of 69:21 between the normal and the iso form. Hence, if the experimental data could fit the iso form, the simulation should have lead to this isomer. A further experiment was performed to exclude the iso form via molecular dynamic simulations in vacuo. As the two different isomers are not interconvertible modified analogues of the three compounds were employed. The two residues forming the transannular bridge were replaced by alanine. For each of the three *S*-deoxo-amaninamides two different starting structure were created; one with a backbone conformation similar to the normal isomer and the other analogous to the iso form. Apart from the distances to the side chains of Trp[4] and Cys[8] all other restraints were used for these calculations. Since both simulations converged for all three compounds to the normal isomer, the existence of the iso form in solution can be safely excluded.

The region of the CD spectra in-between a wavelength of 210 and 260 nm where deviations are detected is related to the

(48) Hoffmann, R. W. *Angew. Chem., Int. Ed. Engl.* **1992**, *31*, 1124−1134.

carbonyls. The initial assumption that these differences may arise from two isomeric forms can be excluded through the performed test calculations. As the normal form of *S*-deoxo-D-Ile[3]-amaninamide shows a CD spectrum similar to compound **1** (l-configuration) the influence of the chirality in this position can also be denied. Therefore, the detected differences in the CD spectra must arise from the discussed turn structures. The βI-turn in compound **1** leads to negative, the βII-turn in **2** to positive values. The Gly[3]-analogue shows a higher flexibility than analogs **1** and **2**. Hence, the resulting CD spectrum lies in-between these of the other two as a result of conformational averaging in the turn region with Hyp[2] in the $i+1$ position. Recent studies have shown that the most frequently occurring types of β-turns (type I and type II) give significantly different CD spectra: βI-turns generally give class C CD spectra and βII-turns result in class B spectra.[49,50] Our interpretation that the differences between the CD spectra of the three analogs are caused by variations of the β-turn structure fits very well to the results given in ref 50. The red-shift of the maxima of about 20 nm compared to the spectra shown therein might be a result of the different solvents. In ref 50 the authors state that an increase in conformational flexibility leads to a decreased band intensity, which corresponds very well to the effect found for compound **3**.

Biological tests show that the inhibitory effect of the three amatoxin analogs on RNA polymerase II of *Drosophila melanogaster* embryos was more than 100 times smaller than that of α-amatoxin. The L-Ala[3]-compound (**1**) showed $K_i = 10^{-5}$ (α-amanitin: $K_i = 10^{-8}$), comparable to that value obtained by the same compound with RNA-polymerase of calf thymus (3×10^{-5}). Surprisingly the D-Ala[3]-analogue (**2**) was about 5 times more inhibitory ($K_i = 5 \times 10^{-6}$) than **1**. This effect might be caused by the methyl of D-Ala[3] group in **2**, which is more exposed compared to **1**. Glycine-analogue **3** exhibited no inhibitory effect, in contrary it seemingly stimulated RNA formation in 10^{-6} mol solution by 10−20% as compared to the control without any addition. As the side chain in position 3 of the three analogues is very short compared to that of the natural amatoxin-peptides, the detected rather small inhibitory activities could be a result of a side chain which is too short.

(49) Hollósi, M.; Majer, Z. S.; Rónai, A. Z.; Magyr, A.; Medzihradszky, K.; Holly, S.; Perczel, A.; Fasman, G. D. *Biopolymers* **1994**, *34*, 177−185.
(50) Perczel, A.; Hollósi, M.; Foxman, B. M.; Fasman, G. D. *J. Am. Chem. Soc.* **1991**, *113*, 9772−9784.

Conclusion

The herein examined *S*-deoxo-amaninamide analogues all appear in the normal form in solution. The backbone is bent and both halves are nearly orthogonal to each other. Each compound exhibits two β-turns with residues 2 and 6 in the $i+1$ position. The conformational differences between the analogues lie in the structure of the turn with Hyp[2] in $i+1$. The Ala[3]-analogue shows a βI-turn in this position, which is further stabilized by an additional hydrogen bond to the Asn[1] sidechain. Its conformation is identical to that found for β-amanitin in the crystal structure. Both of the other compounds show a βII-turn. However, the Gly[3] analogue seems to exhibit a higher flexibility in this region.

Based on the results of conformational analysis we explain the strong differences of the CD spectra in-between a wavelength of 210 and 260 nm with the different types of turns with Hyp[2] in the $i+1$ position. The assumption that these differences may arise from two isomeric forms can be excluded. The βI-turn in compound **1** leads to negative, and the βII-turn in **2** to positive values. As a result of conformational averaging the Gly[3]-analogue shows a decreased band intensity.

Acknowledgment. This contribution is dedicated to Ivar Ugi on the occasion of his 65th birthday.

Supporting Information Available: Tables of carbon chemical shifts, of the experimentally determined NOE values and of the proton−proton distances resulting from the MD calculations for all three compound are available (9 pages). This material is contained in many libraries on microfiche, immediately follows this article in the microfilm version of the journal, can be ordered from the ACS, and can be downloaded from the Internet; see any current masthead page for ordering information and Internet access instructions.

JA9529706